ARTICLE
Journal of Cellular Biochemistry 116:1624–1637 (2015)

Journal of Cellular Biochemistry

FV-429 Induced Apoptosis Through ROS-Mediated ERK2 Nuclear Translocation and p53 Activation in Gastric Cancer Cells

Yuxin Zhou,[1] Libin Wei,[1] Haiwei Zhang,[1] Qinsheng Dai,[1] Zhiyu Li,[1] Boyang Yu,[2] Qinglong Guo,[1]* and Na Lu[1]*

[1]*State Key Laboratory of Natural Medicines, Jiangsu Key Laboratory of Carcinogenesis and Intervention, Key Laboratory of Drug Quality Control and Pharmacovigilance, JiangSu Key Laboratory of Drug Design and Optimization, China Pharmaceutical University, 24 Tongjiaxiang, Nanjing 210009, P.R. China*

[2]*Department of Complex Prescription of TCM, China Pharmaceutical University, Nanjing, P.R. China*

ABSTRACT

Following our previous finding which revealed that FV-429 induces apoptosis in human hepatocellular carcinoma HepG2 cells, in this study, we found that FV-429 could also induce apoptosis in human gastric cancer cells. Firstly, FV-429 inhibited the viability of BGC-823 and MGC-803 cells with IC_{50} values in the range of 38.10 ± 6.28 and 31.53 ± 6.84 μM for 24 h treatment by MTT-assay. Secondly, FV-429 induced apoptosis in BGC-823 and MGC-803 cells through the mitochondrial-mediated pathway, showing an increase in Bax/Bcl-2 ratios, and caspase-9 activation, without change in caspase-8. Further research revealed that the mitogen-activated protein kinases, including c-Jun N-terminal kinase, extracellular regulated kinase, and p38 mitogen-activated protein kinase, could be activated by FV-429-induced high level ROS. Moreover, FV-429 also promoted the ERK2 nuclear translocation, resulting in the co-translocation of p53 to the nucleus and increased transcription of p53-regulated proapoptotic genes. FV-429 significantly inhibited the nude mice xenograft tumors growth of BGC-823 or MGC-803 cells in vivo. J. Cell. Biochem. 116: 1624–1637, 2015.

KEY WORDS: p53; REACTIVE OXYGEN SPECIES; EXTRACELLULAR REGULATED KINASE; NUCLEAR TRANSLOCATION

Gastric cancer (GC) is currently the fourth most common cancer worldwide, and 8% of the newly diagnosed cancer cases are malignancies of the stomach. Over 700,000 people die each year from GC, which makes it the second leading cause for cancer-related deaths [Ferlay et al., 2010]. GC is an asymptomatic disease at early stages and is therefore often detected late; the 5-year survival being only 20–30% [Pedrazzani, 2011]. Although the curative rate for early stage gastric cancer has been increased by improvements in endoscopic [Sugimoto et al., 2012] and surgical techniques [Sano et al., 2004], the prognosis of advanced and unresectable GC remains quite poor [Wagner et al., 2006; Ott et al., 2011; Hayakawa et al., 2012].

Flavonoids are a group of compounds widely distributed in plant sources, such as seeds, citrus fruits, olive oil, as well as tea and red wine. It has long been recognized that flavonoids possess antiinflammatory, antioxidant, antiallergic, hepatic-protective, antithrombosis, and antiviral activities [Havsteen, 1984; Gabor, 1986; Das and Ray, 1988; Kandaswami and Middleton, 1994; Middleton et al., 2000; Aiyegoro and Okoh, 2009]. They are low molecular weight compounds composed of a three-ring structure with various

Yuxin Zhou and Libin Wei contributed equally to this work.

Grant sponsor: State Key Laboratory of Natural Medicines, China Pharmaceutical University; Grant numbers: JKGZ201101, SKLNMZZ201210, SKLNMZZCX201303, SKLNMZZJQ201302; Grant sponsor: Natural Science Foundation of China; Grant numbers: 30973556, 91029744, 81173086; Grant sponsor: Natural Science Foundation of Jiangsu Province; Grant number: BK2011620; Grant sponsor: National Science & Technology Major Project; Grant number: 2012ZX09304-001; Grant sponsor: Program for Changjiang Scholars and Innovative Research Team in University; Grant number: PCSIRT-IRT1193.

*Correspondence to: Qing-Long Guo and Na Lu, State Key Laboratory of Natural Medicines, Jiangsu Key Laboratory of Carcinogenesis and Intervention, Key Laboratory of Drug Quality Control and Pharmacovigilance, JiangSu Key Laboratory of Drug Design and Optimization, China Pharmaceutical University, 24 Tongjiaxiang, Nanjing 210009, P.R. China. E-mail: anticancer_drug@yahoo.com.cn

Manuscript Received: 23 January 2014; Manuscript Accepted: 23 January 2015

Accepted manuscript online in Wiley Online Library (wileyonlinelibrary.com): 3 February 2015

DOI 10.1002/jcb.25118 • © 2015 Wiley Periodicals, Inc.

substitutions [Middleton et al., 2000; Gilman et al., 2002; Pick et al., 2011]. Many flavonoids possess anti-tumor activity against various human cancer cell lines and xenograft systems of human tumors, suggesting that they may be promising anticancer agents [Liu et al., 2010; Garcia-Tirado et al., 2012; Romagnolo and Selmin, 2012]. Some reports showed that flavonoids could regulate the cellular redox, and influence the ROS level [Das et al., 2012].

Reactive oxygen species (ROS) are produced at the highest concentrations within the mitochondria and consist of superoxide anion ($O_2^{-\bullet}$), hydrogen peroxide (H_2O_2), and hydroxyl radicals ($OH^{\bullet}$) [Trachootham et al., 2009]. It is known that ROS play an important role in regulating cell death and differentiation, suggesting their levels need to be tightly regulated for normal development, particularly within the brain. ROS also serve critical signaling roles; hence, their levels must be tightly regulated to avoid cellular damage and dysfunction [Benz and Yau, 2008; Celotto et al., 2012]. It has been previously demonstrated that the accumulation of ROS could cause the loss of membrane potential (MMP) and activates the mitogen activated protein kinase (MAPK) pathway, including the c-Jun N-terminal kinase (JNK) and the p38 pathways that are responsible for ROS-mediated cell apoptosis [Van Laethem et al., 2006; Liu et al., 2011].

The p53 tumor suppressor gene product is a transcription factor that enhances the transcription of several genes known to play a critical role in transducing signals from DNA damage [Lane et al., 1994; Morgan and Kastan, 1997; Shieh et al., 1997; el-Deiry, 1998; Lakin and Jackson, 1999]. Its expression and activity are elevated in response to ionizing radiation, UV light, or certain genotoxic chemicals and mediate DNA repair, cell cycle arrest, and apoptosis [Morgan and Kastan, 1997; el-Deiry, 1998; Lakin and Jackson, 1999; Jiang et al., 2004]. The functional activity of p53 is regulated through transcription, translation, protein turnover, cellular compartmentalization as well as its association with other proteins, such as MDM2 [Shieh et al., 1997; Jiang et al., 2004]. In addition, posttranslational covalent modifications, such as phosphorylation and acetylation of specific amino acids of the p53 protein, have been known to affect p53 activity [Shieh et al., 1997; Siliciano et al., 1997; Meek, 1999].

FV-429 is a newly synthesized flavonoid with bis(2-hydroxyethyl) amino-propoxy substitution [Yang et al., 2011] (Fig. 1A). In this study, we demonstrated that FV-429 exhibited anti-tumor effect in vitro, with the effects of apoptosis induction. FV-429 possesses significant growth inhibitory effects on various cancer cell lines especially on gastric cancer cells. In addition, apoptotic pathways induced by FV-429 are associated with the elevation of the ratio of Bax/Bcl-2 and the activation of caspase family proteins. Moreover, we provided evidence of FV-429 antitumor activity by the induction of ERK2 and translocation of p53 into the nucleus driven by increasing cellular ROS levels. Taken together, our results provide evidences that FV-429 is a novel and potent anti-tumor agent for malignant gastric cancer therapy.

MATERIALS AND METHODS

CELL CULTURE

BGC-823 cells and MGC-803 were cultured in RPMI 1640 culture medium (Gibco, USA) supplemented with 10% fetal bovine serum, 0.2% sodium bicarbonate, 100 units/ml penicillin and 100 μg/ml streptomycin in a humidified 5% CO_2 atmosphere at 37°C.

ANIMALS

Female athymic BALB/c nude mice (5–6 weeks old) with body masses ranging from 18 to 22 g were supplied by Shanghai Laboratory Animal Limited Company. Animals were maintained in a pathogen-free environment (23 ± 2°C and 55 ± 5%humidity) on a 12 h light–12 h dark cycle with food and water supplied ad libitum throughout the experimental period. This experiment was conducted in accordance with the guideline issued by the State Food and Drug Administration (SFDA of China).

REAGENTS AND ANTIBODIES

FV-429 and wogonin were obtained from Dr. Zhiyu Li (China Pharmaceutical University, China). FV-429 is a derivative of wogonin. FV-429 and wogonin were dissolved in DMSO, stored at −20°C, and diluted with medium before each experiment. The final DMSO concentration did not exceed 0.1% throughout the study. Antibodies of β-actin, caspase-3, -8, -9, Bcl-2, Bax, JNK, p-JNK, p38, p-p38, ERK1/2, p-ERK1/2, and Histone were purchased from Santa Cruz (Santa Cruz, CA). Antibodies of p53 and phospho-p53 (Ser15) were purchased from Cell Signaling Technology (Beverly, MA) [Fazal et al., 2005; Qiang et al., 2008; Li et al., 2009]. IRDye™ 800 conjugated anti-mouse and anti-rabbit second antibodies were obtained from Rockland Inc. (Philadelphia, PA). 4,6-Diamino-2-phenyl indole (DAPI) was purchased from Santa Cruz (Santa Cruz, CA). MTT [3-(4,5-dimethylthiazol-2-yl)-2,5-diphenytetrazoliumbromide] was obtained from Fluka chemical corp (Ronkonkoma, NY) and was dissolved in 0.01 M PBS. All other chemicals were of the highest pure grade available. N-Acetyl-L-cysteine (NAC, the scavenger of ROS), and U0126 (an inhibitor of ERK), were obtained from Beyotime Institute of Biotechnology (Haimen, China).

CELL VIABILITY ASSAY

Several tumor cell lines were plated in the appropriate media on 96-well plates in a 100 μl total volume at an optimum density. Cells were treated with FV-429 at different concentration ranging from 3.6 to 100 μM. The plates were incubated at 37°C in 5% CO_2 for 24 h. After that, FV-429 exposure for BGC-823 and MGC-803 cells at different time points, including 24, 48, and 72 h. Cell viability was determined based on mitochondrial conversion of MTT to formazan. The absorbance (A) was measured at 570 nm. Inhibition ratio (%) was calculated using the following equation:

$$\text{Inhibition ratio}\,(\%) = [(A_{control} - A_{treated})/A_{control}] \times 100\%$$

$A_{treated}$ and $A_{control}$ are the average absorbance of three parallel experiments from treated and control groups, respectively.

IC_{50} was taken as the concentration that caused 50% inhibition of cell viability and calculated by the Logit method [Fazal et al., 2005; Wang et al., 2007].

CELL MORPHOLOGICAL ASSESSMENT

To detect morphological evidence of apoptosis, cell nuclei were visualized following DNA staining with the fluorescent dye DAPI.

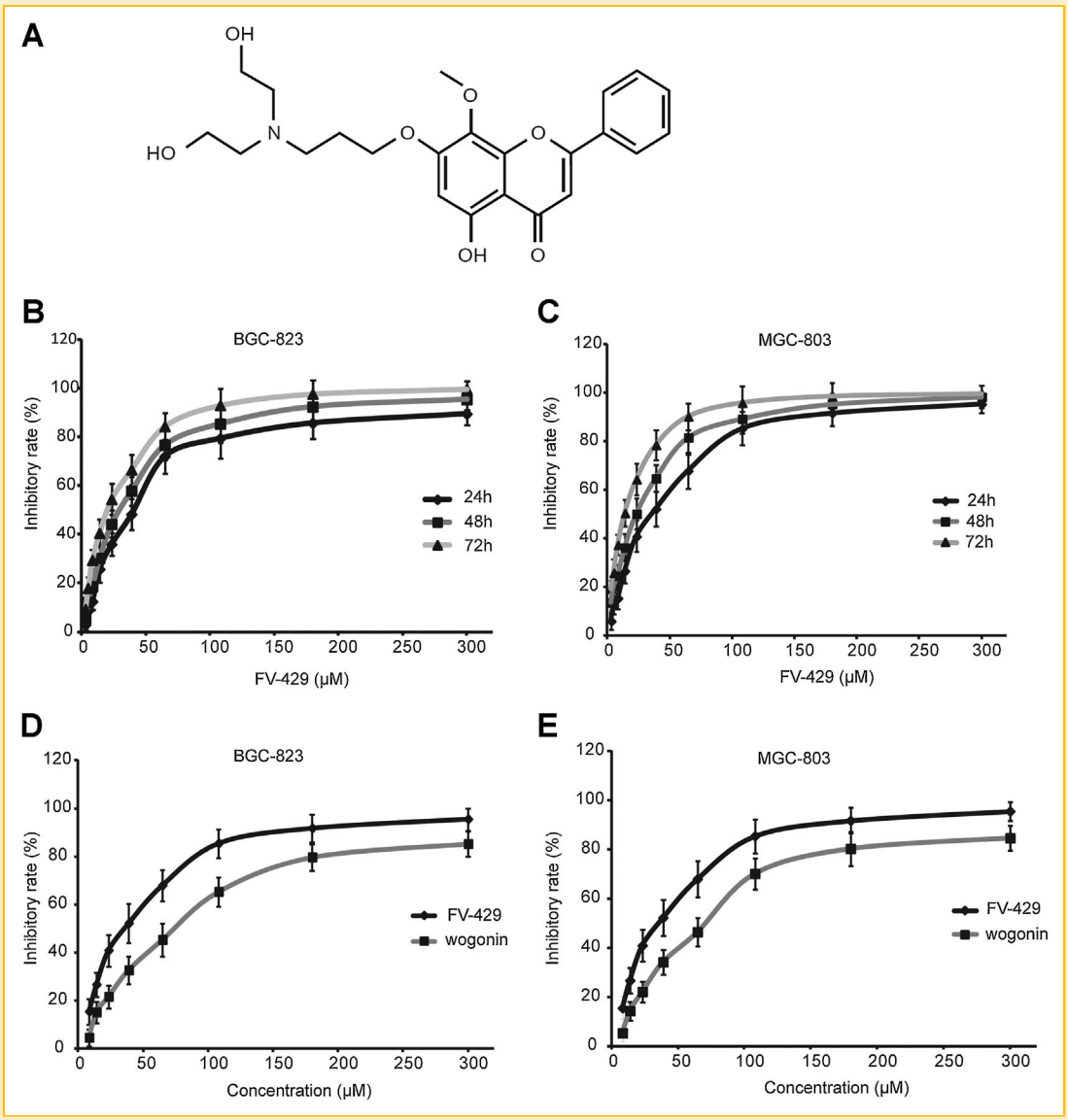

Fig. 1. FV-429 inhibits the viability of various tumor cell lines. A: Molecular structure of FV-429 ($C_{23}H_{25}NO_7$, molecular weight = 429). B: The inhibitory effect of FV-429 on BGC-823 cells with different concentrations for 24, 48, and 72 h. C: The inhibitory effect of FV-429 on MGC-803 cells with different concentrations for 24, 48, and 72 h. D: BGC-823 cells were treated with different concentrations of FV-429 and wogonin for 24 h. E: MGC-803 cells were treated with different concentrations of FV-429 and wogonin for 24 h. Data were shown as mean ± SEM (n = 3).

After treatment with FV-429 for 48 h, cells were fixed with 4% paraformaldehyde for 20 min and washed with PBS twice, and then incubated with 0.3% Triton X-100 (in PBS) for 10 min at room temperature. After washed with PBS twice, cells were incubated with DAPI for 10 min and then observed using fluorescent microscopy (Olympus, Japan) with a peak excitation wavelength of 340 nm [Shi et al., 2008; Wang et al., 2006].

ANNEXIN V/PI DOUBLE STAINING ASSAY

Apoptosis-mediated cell death of tumor cell was examined using a double staining method with FITC-labeled Annexin V/PI Apoptosis Detection kit (Biovision, CA) according to the manufacturer's instructions. Flow cytometric analysis was performed 10–15 min after supravital staining. Data acquisition and analysis were performed in a Becton Dickinson FACSCalibur flow cytometer using CellQuest software (BD Biosciences, Franklin Lakes, NJ). The lower left section of fluorocytogram (Annexin V−, PI−) represents the normal cells, lower right section of fluorocytogram (Annexin V+, PI−) represents early and median apoptosis cells, upper right section of fluorocytogram (An+, PI+) represents late apoptosis cells [Jalving et al., 2006; Liu et al., 2007].

MEASUREMENT OF H_2O_2

Generation of ROS was assessed by using the fluorescent signal 2,7-dichlorodihydrofluorescein (H_2DCFDA), a cell-permeable indicator for ROS initially shown to react with H_2O_2. The BGC-823 and MGC-803 cells were pretreated with different concentrations of FV-429 (10, 15, and 20 μM) for 48 h. The cells were incubated with H_2DCFDA

(100 μM) in PBS for 30 min. After 30 min at 37°C, 2,7-dichlorofluorescein fluorescence (excitation of 485 nm and emission of 525 nm) was observed under a fluorescent microscope (Olympus IX51, Japan). The fluorescence intensity was measured using flow cytometry (FACSCalibur, Becton Dickinson), and was analyzed by the software Modfit and CellQuest (BD Biosciences, Franklin Lakes, NJ) with settings at excitation and emission equal to 488/525 nm [Bobyleva et al., 1998].

MEASUREMENT OF $^{\bullet}O_2$ LEVEL

FV-429-treated (10, 15 and 20 μM for 48 h) cells were harvested and stained with 5 μM $^{\bullet}O_2^-$-sensitive dye dihydroethidium (DHE, Beyotime Institute of BioTechnology, Haimen, China) for 60 min at 37°C in the dark. Subsequently, cells were washed three times with PBS (2,000 rpm × 5 min), and the fluorescence intensity was assayed by FACSCalibur flow cytometry (Becton Dickinson, San Jose, CA) at Ex./Em. = 300 nm/610 nm.

WESTERN BLOTTING ANALYSIS

Cells were treated with indicated concentration of FV-429 for 24 h, and then cells were collected and lysed in lysis buffer (100 mM Tris–Cl, pH 6.8, 4% (m/v) sodium dodecylsulfonate, 20% (v/v) glycerol, 200 mM beta-mercaptoethanol, 1 mM phenylmethylsulfonyl fluoride, and 1 g/ml aprotinin). Lysates were centrifuged at 12,000*g* for 30 min at 4°C. The concentration of total proteins was measured using the BCA assay method with Varioskan spectrofluorometer and spectrophotometer (Thermo, Waltham, MA) at 562 nm. Protein samples were separated with 12% SDS–PAGE gel and transferred onto the PVDF membranes (Millipore, Billerica, MA). Immune complexes were formed by incubation of the following antibodies: anti-caspase-3, anti-caspase-8, anti-caspase-9, anti-Bcl-2, anti-Bax, anti-JNK, anti-p-JNK, anti-p38, anti-p-p38, anti-ERK1/2, anti-p-ERK1/2, anti-p53, anti-p-p53(ser-15), and β-actin for 1 h at 37°C; followed by IRDyeTM 800 conjugated second antibody for 1 h at 37°C. Immunoreactive protein bands were detected with an Odyssey Scanning System (Li-COR Inc., Superior St. Lincoln, NE). All blots were stripped and reprobed with anti-β-actin antibody to ascertain equal loading of proteins [Nirmalan et al., 2009].

EXTRACTION OF CYTOPLASMIC AND NUCLEAR FRACTIONS

About 1×10^7 cells were collected and washed twice with ice-cold PBS. The harvested cells were lysed in nuclear protein extraction buffer A (Boster Biological Technology, Wuhan, China) on ice for 30 min. Then the cell lysates were centrifuged at 12,000*g* for 10 min at 4°C and the supernatant was collected as the cytoplasmic fractions. The pellet was lysed in nuclear protein extraction buffer B (Boster Biological Technology) on ice for 30 min. Then the lysates were centrifuged at 12,000*g* for 10 min at 4°C and the supernatant was collected as the nuclear fractions. PMSF and leupeptin were added into buffer A and buffer B before use.

IMMUNOFLUORESCENCE AND CONFOCAL FLUORESCENCE MICROSCOPY

Cells were fixed with 4% paraformaldehyde in PBS at 1-h intervals, permeabilized with 0.5% Triton X-100, and blocked with 3% BSA for 30 min. Incubation with primary antibodies (diluted 1:50) (Abcam Ltd., HK, China) against ERK2 was done overnight at 4°C. Mitochondrial were visualized with Mitotracker Red (Molecular Probes, Inc., Eugene, OR), incubated at a final concentration of 150 nM for 45 h at 37°C. Then the nuclei were stained with 4′,6-diamidino-2-phenylindole (DAPI, Sigma–Aldrich, St. Louis, MO) 20 minutes before imaging. A laser scanning confocal microscope FV10-ASW [Ver 2.1] (Olympus Corp, MPE FV1000) was used for co-localization analysis.

IMMUNOPRECIPITATION

Nuclear fractions were extracted as described above. Bradford Assay was used to determine the protein concentration. Sufficient amount of p53 antibody was added into 200 μg proteins and gently rotated at 4°C overnight. The immunocomplex was captured by adding 25 μl protein G-agarose beads (Santa Cruz, CA) and gently rotating at 4°C for 3 h. Then the mixture was centrifuged at 1500*g* for 5 min at 4°C and the supernatant was discarded. The precipitate was washed for three times with ice-cold RIPA buffer, resuspended in 3× sample buffer and boiled for 5 min to dissociate the immunocomplex from the beads. The supernatant was collected by centrifugation and subjected to Western blot (8% SDS–PAGE).

INHIBITORY EFFECTS ON BGC-823 AND MGC-803 NUDE MICE XENOGRAFTS

This experiment was conducted in accordance with the guideline issued by the State Food and Drug Administration (SFDA of China). Forty nude mice were inoculated subcutaneously with injections of 1×10^6 MGC-823 and BGC-803 cells/mouse into the right axilla. After 7 days of growing, tumor sizes were determined using micrometer calipers, and the nude mice with similar tumor volume (mice with tumors that were too large or too small were eliminated) were randomly divided into the following five groups (six mice/group): saline control group, FV-429 40 mg/kg every 2 days group, FV-429 20 mg/kg every 2 days group, FV-429 10 mg/kg every 2 days group and 5-Fu 20 mg/kg every 2 days group. Tumor sizes were measured every 3 days using micrometre calipers and tumor volume was calculated using the following formula: TV $(mm^3) = d^2D/2$, where d and D were the shortest and the longest diameter, respectively.

STATISTICAL ANALYSIS

All results shown represent mean ± SEM from triplicate experiments performed in a parallel manner unless otherwise indicated. Statistical analyses are performed using one-way analysis of variance (ANOVA), followed by the Bonferroni posttest for multiple group comparisons. All comparisons are made relative to untreated controls and significance of difference is indicated as $^{*}P < 0.05$ and $^{**}P < 0.01$.

RESULTS

FV429 INHIBITS CELL VIABILITY IN TUMOR CELLS

MTT assay was used to investigate the inhibitory effect of FV-429 on gastric cancer cells. Upon treatments for 24 h, FV-429 inhibited the viability of BGC-823 and MGC-803 cells effectively. The IC_{50} values

of FV-429 on BGC-823 cells were 38.10 ± 6.28, 31.98 ± 5.42, and 25.64 ± 6.38 μM, obtained for 24, 48, and 72 h treatment, respectively (Fig. 1B); and on MGC-803 cells were 31.53 ± 6.84, 26.43 ± 4.19, and 20.89 ± 5.08 μM, for 24, 48, and 72 h treatment, respectively (Fig. 1C). And the IC_{50} values of wogonin in BGC-823 and MGC-803 cells were 68.66 ± 8.62 and 65.90 ± 7.29 μM, obtained for 24 h treatment (Fig. 1D and E). We found FV-429 has lower IC_{50} values than wogonin. The results suggested that FV-429 inhibited the growth of BGC-823 and MGC-803 cells in a time- and concentration-dependent manner.

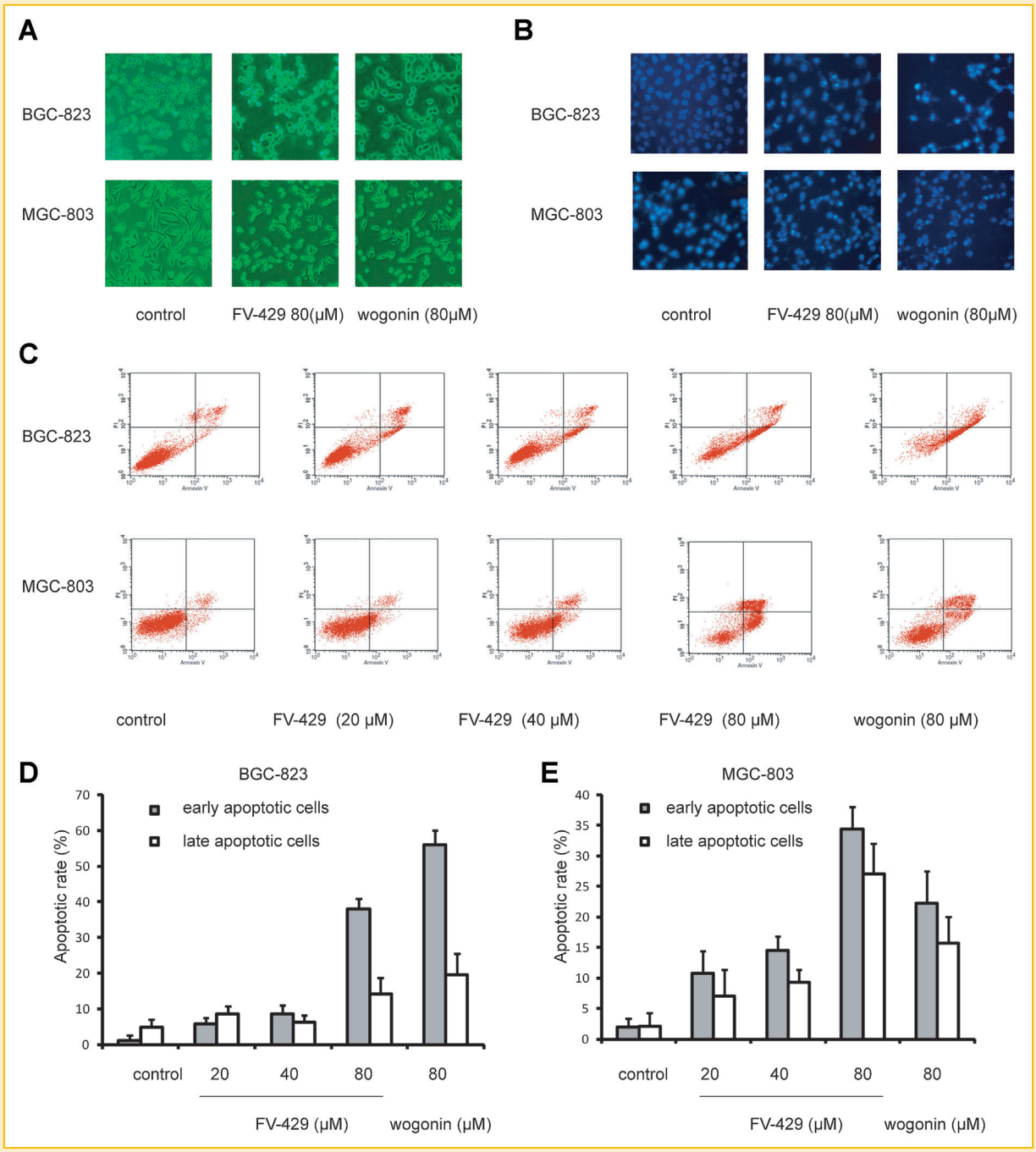

Fig. 2. FV-429 induces apoptosis in BGC-823 and MGC-803 cells. BGC-823 and MGC-803 cells were treated with 20, 40 and 80 μM FV-429 and 80 μM wogonin for 24 h. A: Morphological change of BGC-823 and MGC-803 cells were observed under an inverted light microscope (200×). B: Nucleolus morphologic changes were observed by fluorescent microscope (400×). The nuclei exhibited bright condensed chromatin. The white arrows indicate the apoptotic cells with nuclear fragments. C: Annexin V/PI double-staining assay of BGC-823 and MGC-803 cells. Y Axis showed PI labeled population and X axis showed FITC-labeled Annexin V positive cells. D: The apoptotic rates of BGC-823 cells induced by FV-429 and wogonin. E: The apoptotic rates of MGC-803 cells induced by FV-429 and wogonin. Values are each the mean ± SEM (n = 3). $^{*}P < 0.05$, $^{**}P < 0.01$, significant difference from the control.

FV-429 INDUCES APOPTOSIS IN BGC-823 AND MGC-803 CELLS

After the cells were treated by FV-429 or wogonin for 24 h, the shape of BGC-823 and MGC-803 cells were distorted severely (Fig. 2A). To assess whether FV-429 could induce apoptotic cell death, the nuclei changes in BGC-823 and MGC-803 cells were observed under a fluorescent microscope, staining with fluorochrome dye DAPI. As a result, untreated BGC-823 and MGC-803 cells were stained equably with blue fluorescence, demonstrating the steady chromatinic distribution in nucleolus, instead FV-429-treated BGC-823 and MGC-803 cells emitted bright fluorescence, the early phenomena of apoptosis, due to the chromatin congregation and the nucleolus pyknosis. At the concentration of FV-429 (40 and 80 μM) and wogonin (80 μM), cellular nucleus of BGC-823 and MGC-803 cells disintegrated and formed many nuclear fragments (Fig. 2B). These results suggested that FV-429 could induce apoptosis in BGC-823 and MGC-803 cells.

To further confirm the apoptosis induced by FV-429, Annexin V/PI staining assay was used. After cells were treated with 20, 40, and 80 μM FV-429 or 80 μM wogonin for 24 h, the early apoptotic rates were 5.73%, 8.68%, 38.1%, and 55.88%, respectively, and the late apoptotic rates were 8.58%, 6.19%, 14.12%, and 19.61% in BGC-823 cells, respectively (Fig. 2C–E). Meanwhile, after cells were treated with 20, 40, and 80 μM FV-429 or 80 μM wogonin for 24 h, the early apoptotic rates were 10.75%, 14.47%, 34.38%, and 22.16%, respectively, and the late apoptotic rates were 7.05%, 9.26%, 26.99%, and 15.77% in MGC-803 cells. These results suggested that FV-429 induced apoptosis in BGC-823 and MGC-803 cells in a concentration-dependent manner. We found the FV-429 had the same apoptosis-inducing effects as wogonin under a lower concentration.

FV-429 INDUCED APOPTOSIS THROUGH MITOCHONDRIAL-MEDIATED APOPTOTIC PATHWAY AND INCREASED CELLULAR ROS LEVEL

It has been reported that wogonin has potent antitumor activity by inducing a mitochondrial-mediated apoptosis [Yu et al., 2007; Lin et al., 2011]. To further investigate whether FV-429, the derivative of wogonin, induced apoptosis through mitochondria-mediated pathway, the levels of intracellular ROS in BGC-823 and MGC-803 cells were measured by flow cytometry. As shown in Figure 3A and B, compared with untreated cells, the treatment of FV-429 for 24 h resulted in a conspicuous and concentration dependent increase in $\cdot O_2^-$ and H_2O_2 levels. We also found that the FV-429 should increase the level of $\cdot O_2^-$ and H_2O_2 in MGC-803 cells (Fig. 3C, D).

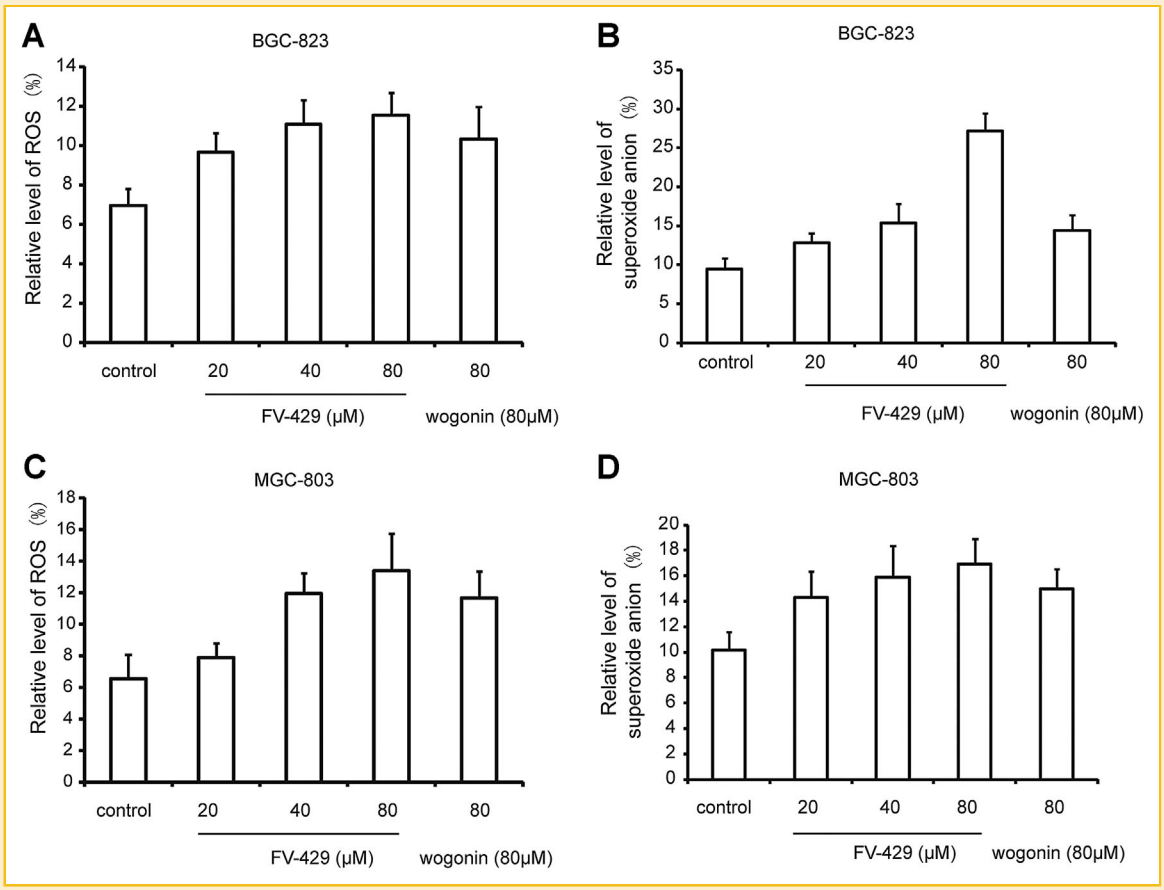

Fig. 3. Effects of FV-429 on the ROS of BGC-823 and MGC-803 cells. A: The level of intracellular reactive oxygen species (ROS) in BGC-823 cells was measured by flow cytometry. B: The level of intracellular superoxide anion in BGC-823 cells was measured by flow Cytometry. C: The level of intracellular reactive oxygen species (ROS) in MGC-803 cells was measured by flow cytometry. D: The level of intracellular superoxide anion in MGC-803 cells was measured by flow cytometry. Data were shown as mean ± SEM (n = 3).

Results showed that the FV-429 increased the level of ROS in BGC-823 and MGC-803. Western blot results showed that after BGC-823 and MGC-803 cells were treated with FV-429 and wogonin for 24 h, the expression of Bcl-2 and Bax were changed (Fig. 4A, B). We found that Bcl-2 was decreased while Bax was increased, leading to a raise in the Bax/Bcl-2 ratio (Fig. 4C, D). Caspase-9 and caspase-3 were cleaved to activate significantly after FV-429 treatment for 24 h in BGC-823 cells and PARP cleavage was also observed, indicating that mitochondrial pathway was involved in FV-429-induced apoptosis. However, there was no considerable change in expression of procaspase-8 after the treatment of FV-429.

These results suggested that FV-429 could induce a mitochondrial-mediated apoptotic pathway in BGC-823 and MGC-803 cells.

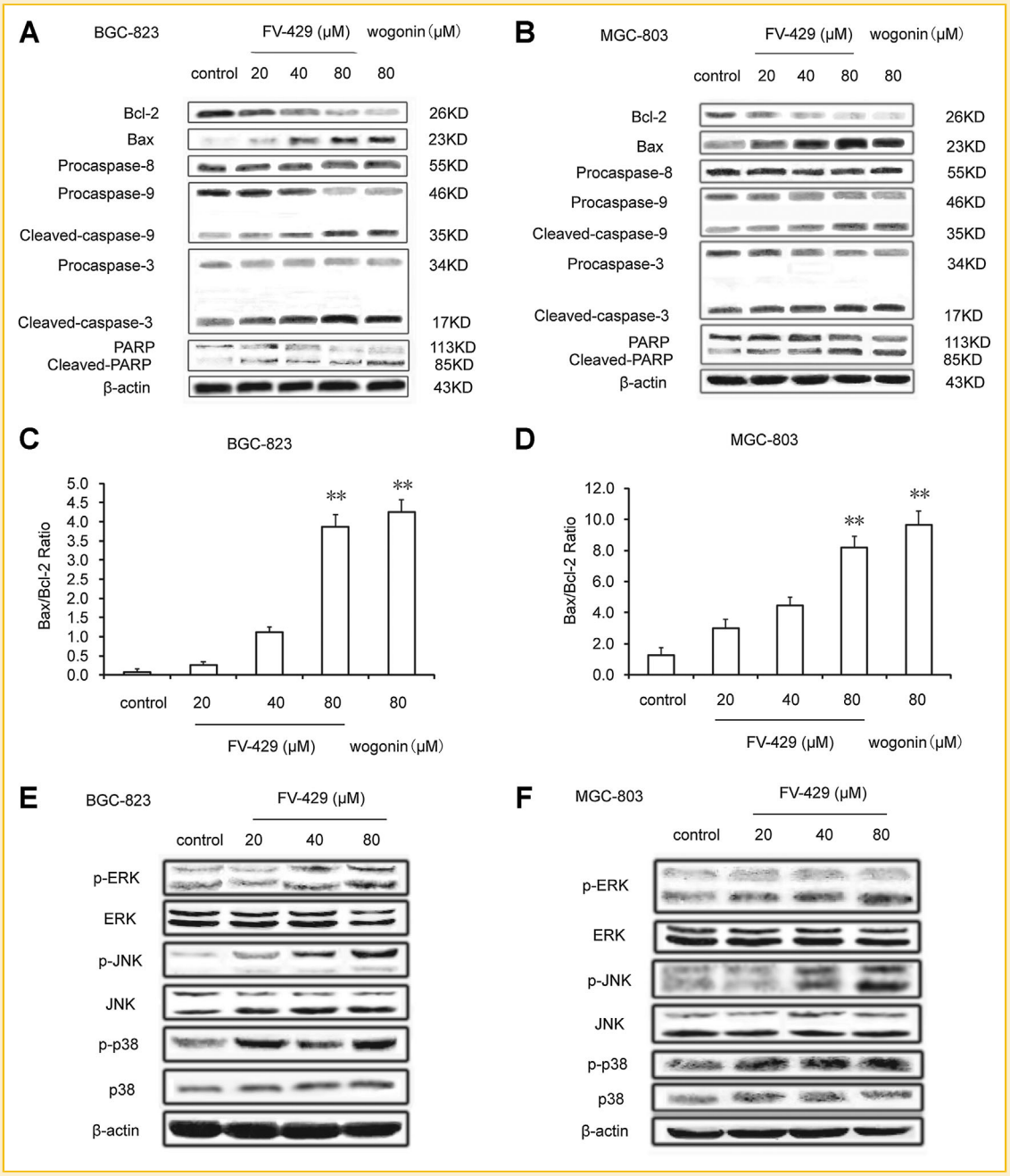

Fig. 4. Effects of FV-429 on apoptosis-related proteins. A: Western blotting analysis of Bcl-2, Bax, caspase-8, -9,-3 and PARP of the BGC-823 cells treated with 20, 40, and 80 μM of FV-429 and 80 μM wogonin for 24 h. B: Western blotting analysis of Bcl-2, Bax, caspase-8, -9,-3 and PARP of the MGC-803 cells treated with 20, 40 and 80 μM of FV-429 and 80 μM wogonin for 24 h. C: A remarkable Bcl-2/Bax ratio increasing was demonstrated in BGC-823. D: A remarkable Bcl-2/Bax ratio increasing was demonstrated in MGC-803. E: Western blotting analysis of ERK, p-ERK, JNK, p-JNK, P38 and p-P38 of the BGC-823 cells treated with 20, 40, and 80 μM of FV-429 for 24 h. F: Western blotting analysis of ERK, p-ERK, JNK, p-JNK, P38 and p-P38 of the MGC-803 cells treated with 20, 40, and 80 μM of FV-429 for 24 h.

MITOGEN-ACTIVATED PROTEIN KINASE PATHWAY MAY BE INVOLVED IN THE APOPTOSIS INDUCED BY FV-429

It has been reported that the accumulation of ROS could activates MAPK pathway, including the JNK and the p38 pathways that are responsible for ROS-mediated cell apoptosis. Here, we investigated the activation of the MAPK pathway in gastric cancer cells upon the treatment of 24 h FV-429. The results showed that the levels of phosphorylated JNK, ERK, and p38 were increased, whereas the level of ERK was decreased in BGC-823 and MGC-803 cells (Fig. 4E, F). Meanwhile, the expression of JNK, ERK, and p38 were not changed upon the treatment of FV-429 in BGC-823 and MGC-803 cells. The results establish that FV-429 could activate the MAPK pathway in BGC-823 and MGC-803 cells.

FV-429-INDUCED NUCLEAR TRANSLOCATION OF ERK2 THROUGH ROS

Moreover, though the compound FV-429 affected the activation of the three members of MAPK family (ERK, JNK, and p38), only ERK and JNK were reported to have the nuclear translocation capacity. To define the detailed the influence of ROS in ERK, we extracted cytoplasmic and nuclear fractions of BGC-823 and MGC-803 cells, and detected distribution of ERK2 between these two compartments. A remarkable translocation of total ERK2 and phosphorylated ERK2 traveled into the nucleus from the cytoplasm were observed in BGC-823 and MGC-803 cells treated with FV-429 (Fig. 5A, C). The nuclear translocation of ERK by FV-429 was abrogated by ROS scavenger NAC (Fig. 5B, D), indicating that the ROS increased by FV-429 was an important regulator of ERK. This was further confirmed by immunofluorescent staining, through the co-localization of ERK2 and DAPI in the merged image after FV-429 treatment, which was cancelled by NAC (Fig. 5E, F). Our results suggest FV-429-induced nuclear translocation of ERK2 through ROS.

FV-429 INDUCED THE CO-NUCLEAR TRANSLOCATION OF p53 WITH ERK2, AND ACTIVATED NUCLEAR p53 VIA THE PHOSPHORYLATION MEDIATED BY ERK

We inferred from the results described above that there must be a link between ERK2 translocation and p53 activation. We extracted nuclear fractions of cells and detected the phosphorylation level of p53 (Ser15). p53 phosphorylation was stimulated by FV-429 for 24 h, while total nuclear p53 remained constant in BGC-823 and MGC-803 cells (Fig. 6A, B). However, the phosphorylation of p53 was thoroughly abolished by ERK inhibitor U0126 (Fig. 6C, D), indicating ERK was responsible for this regulation. p53 is a key transcription factor and regulated many proapoptotic proteins, such as Bax and PUMA. ERK inhibitor U0126 reversed the FV-429-induced expression of PUMA as well. Moreover, we performed Annexin V/PI double-staining assay of BGC-823 and MGC-803 cells treated with FV-429 (60 μM) alone or with U0126 (ERK inhibitor). As shown in Figure 6 E and F, the results suggest that apoptosis induction of FV-429 could be partly inhibited by ERK inhibitors. We found that FV-429 could cause p53 accumulation in the nucleus by immunofluorescent staining in BGC-823 and MGC-803 cells (Fig. 6G, H). It has been reported that nuclear translocation of ERK2 could activate one or more transcription factors, such as p53 [Li et al., 2010]. Subsequently we performed immunoprecipitation of nuclear fractions with p53 antibody and detected the influences of FV-429 on the interactions of p53 with ERK. The results showed that FV-429 increased the binding between p53 and ERK2 in the nucleus (Fig. 6I, J).

FV-429 INHIBITS THE GROWTH OF NUDE MICE XENOGRAFT TUMORS

The in vivo study aimed to examine the effect of FV-429 and was performed by xenografted model. We transplanted BGC-823 or MGC-803 cells into BALB/c nude mice by intravenous injection. The tumor volume measurement further confirmed the significant reduction in the treatment group ($P < 0.01$). After treatment for 21 days, FV-429 (20 and 40 mg/kg), and wogonin (60 mg/kg) showed significant inhibitory effects on the tumor growth (tumor weight and tumor volume) in mice inoculated BGC-823 cells or MGC-803 cells (Fig. 7A–D). In the mice inoculated BGC-823 cells, the inhibitory rates were $67.17 \pm 6.41\%$, $58.58 \pm 7.61\%$, and $61.44 \pm 7.63\%$, respectively in groups of 5-Fu (20 mg/kg), FV-429 (40 mg/kg), and wogonin (60 mg/kg) (Fig. 7E); and in mice inoculated MGC-803 cells, the inhibitory rates of 5-Fu (20 mg/kg), FV-429 (40 mg/kg), and wogonin (60 mg/kg) were $73.31 \pm 6.41\%$, $66.99 \pm 6.72\%$, and $62.25 \pm 5.84\%$, respectively. These results demonstrated that FV-429 was more effective than wogonin on gastric tumor inhibition in vivo. Moreover, FV-429 suppressed tumor growth at a dose of 60 mg/kg to an extent without any significant changes of body weight, whereas the weight of mice was significantly reduced by 5-Fu (20 mg/kg) (Fig. 7G, H).

DISCUSSION

FV-429 is a newly synthesized flavonoid with a bis(2-hydroxyethyl) amino-propoxy substitution. Previous research has revealed apoptosis induced by FV-429 in HepG2 cells [Yang et al., 2011]. FV-429 is a derivative of wogonin. It has been reported that wogonin has anti-tumor effect. FV-429 showed better anticancer effects than wogonin. In this study, we have provided evidence that FV-429 induced mitochondrial-mediated apoptosis, increased ROS levels, and leaded to p53 activation through the co-nuclear translocation with ERK2 and the phosphorylation mediated by ERK in BGC-823 and MGC-803 cells.

Apoptosis, a form of programmed cell death, is characterized by a variety of morphological features, such as loss of membrane asymmetry, cell shrinkage and chromosomal DNA fragmentation [Kerr et al., 1972; Reed, 2000; Lenz, 2004]. In this study, BGC-823 and MGC-803 cells incubated with FV-429 caused cytoplasmic shrinkage and nuclear chromatin condensation in BGC-823 and MGC-803 cells. FV-429 could efficiently induce apoptosis in BGC-823 and MGC-803 cells. The apoptotic rate reached 52.22% and 64.88% after incubation with 80 μM FV-429 in BGC-823 cells and MGC-803 cells. Apoptotic induction by FV-429 was more effective than that of wogonin in BGC-823 and MGC-803 cells upon the same concentration. Moreover, the strong tumor cell inhibition properties of FV-429 prompted us to evaluate its efficacy to inhibit the tumor growth in vivo. A nude mice model bearing inoculated BGC-823 or MGC-803 tumor was used to evaluate the antitumor effect of FV-429 in vivo. The study showed that FV-429 suppressed tumor growth significantly. The rates of inhibition at dose of 40, 20, and 10 mg/kg were 58.58%, 46.32% and 30.11%, and

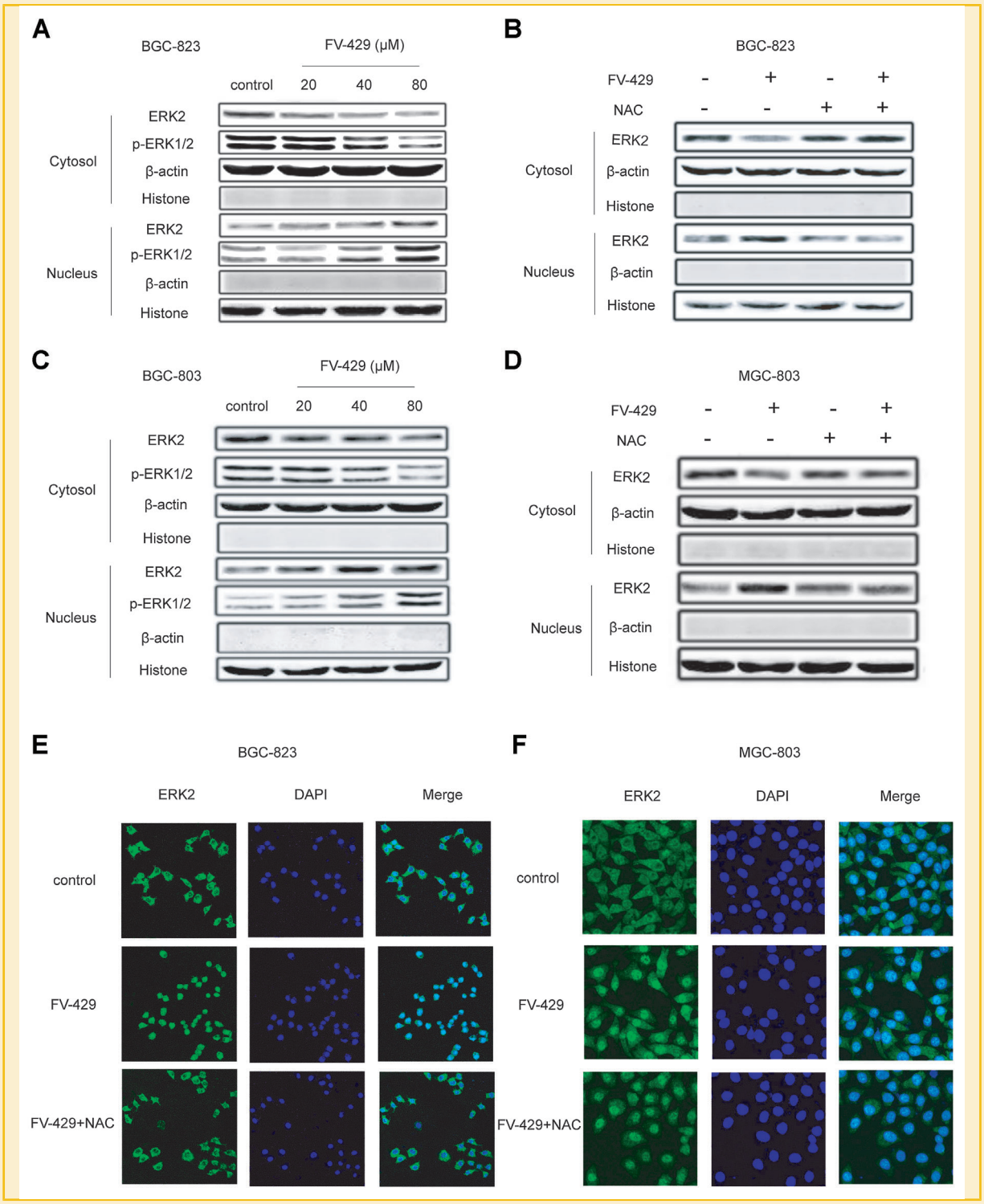

Fig. 5. FV-429-induced nuclear translocation of ERK2 through ROS. A: Nuclear translocation of ERK2 induced by FV-429. Cells were treated with FV-429 (20, 40, and 80 μM). Then cytoplasmic and nuclear fractions were extracted and ERK2 as well as p-ERK1/2 were detected by Western blot. β-Actin and Histone were used as loading control of cytoplasmic and nuclear proteins respectively in BGC-823 cells. B: Effect of ROS scavenger on ERK2 translocation at 24 h. Cells were pretreated with or without NAC (800 μM) for 1 h before FV-429 (80 μM) exposure for 12 h. Then cytoplasmic and nuclear fractions were extracted and ERK2 was detected by Western blot in BGC-823 cells. (C) Nuclear translocation of ERK2 induced by FV-429. Cells were treated with FV-429 (20, 40, and 80 μM). Then cytoplasmic and nuclear fractions were extracted and ERK2 as well as p-ERK1/2 were detected by Western blot. β-Actin and Histone were used as loading control of cytoplasmic and nuclear proteins respectively in MGC-803 cells. (D) Effect of ROS scavenger on ERK2 translocation at 24 h. Cells were pretreated with or without NAC (800 μM) for 1 h before FV-429 (80 μM) exposure for 12 h. Then cytoplasmic and nuclear fractions were extracted and ERK2 was detected by Western blot in MGC-803 cells. E, F: Nuclear translocation of ERK2 was demonstrated by immunofluorescent staining. BGC-823 and MGC-803 cells were pretreated with or without NAC (800 μM) for 1h before FV-429 (80 μM) exposure for 12 h, then ERK2 was immunostained with its primary antibody and FITC conjugated secondary antibody (green). The nucleus was labeled with DAPI (blue). The data were representative of at least three separate experiments.

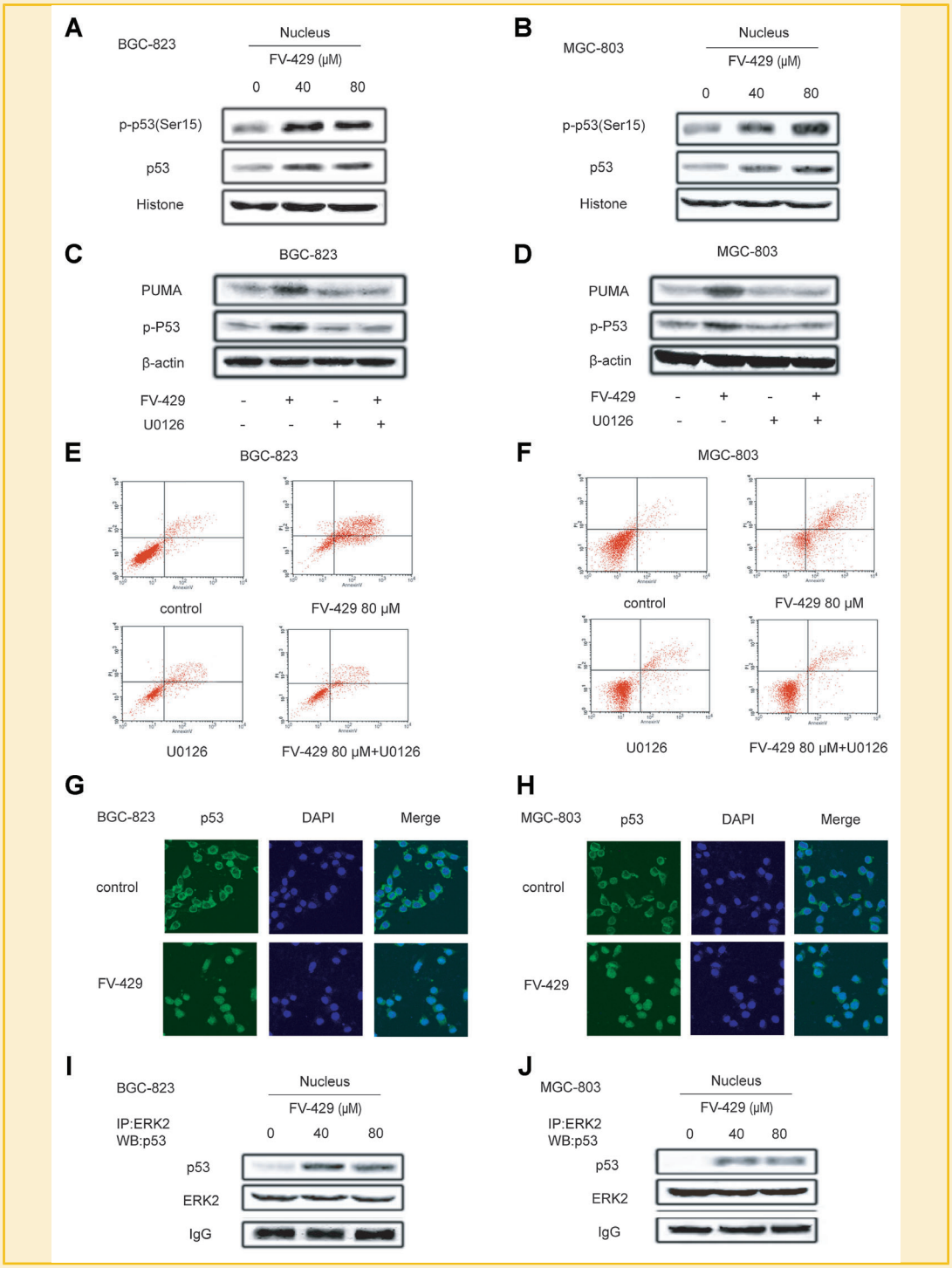

Fig. 6. FV-429 phosphorylated and activated nuclear p53 via ERK2 after the co-nuclear translocation with ERK. A: Phosphorylation of nuclear p53 (Ser15) induced by FV-429. BGC-823 Cells were treated with seleniteFV-429 (40 and 80 μM) as indicated before nuclear fractions were extracted. Then p-p53 (Ser15) and total p53 were detected by Western blot. Histone was used as loading control of nuclear proteins. B: Phosphorylation of nuclear p53 (Ser15) induced by FV-429. MGC-803 Cells were treated with seleniteFV-429 (40 and 80 μM) as indicated before nuclear fractions were extracted. Then p-p53 (Ser15) and total p53 were detected by Western blot. Histone was used as loading control of nuclear proteins. C, D: Cells were treated with FV-429 (80 mmol/l) alone or with U0126 (10 mM, ERK MAPK inhibitor), then the apoptotic rates were identified by flow cytometry. E, F: Effect of U0126 on the expressions of PUMA and p-p53. Cells were pretreated with or without U0126 (10 mM) for 1.5 h before FV-429 (80 μM) exposure for 24 h. Then PUMA and p-p53 were detected by Western blot. G, H: Nuclear translocation of p53 was demonstrated by immunofluorescent staining. BGC-823 and MGC-803 cells were pretreated with FV-429 (80 μM) for 24 h, then p53 was immunostained with its primary antibody and FITC conjugated secondary antibody (green). The nucleus was labeled with DAPI (blue). The data were representative of at least three separate experiments. I, J: Interactions of p53 with ERK2 in the nucleus. BGC-823 and MGC-803 Cells were treated with seleniteFV-429 (40 and 80μM) for 24 h as indicated. Then nuclear fractions were extracted and immunoprecipitated with p53 antibody, after which p53, ERK2 in the immunoprecipitated products were detected by Western blot. IP, immunoprecipitation; WB, Western blot. The data were representative of at least three separate experiments.

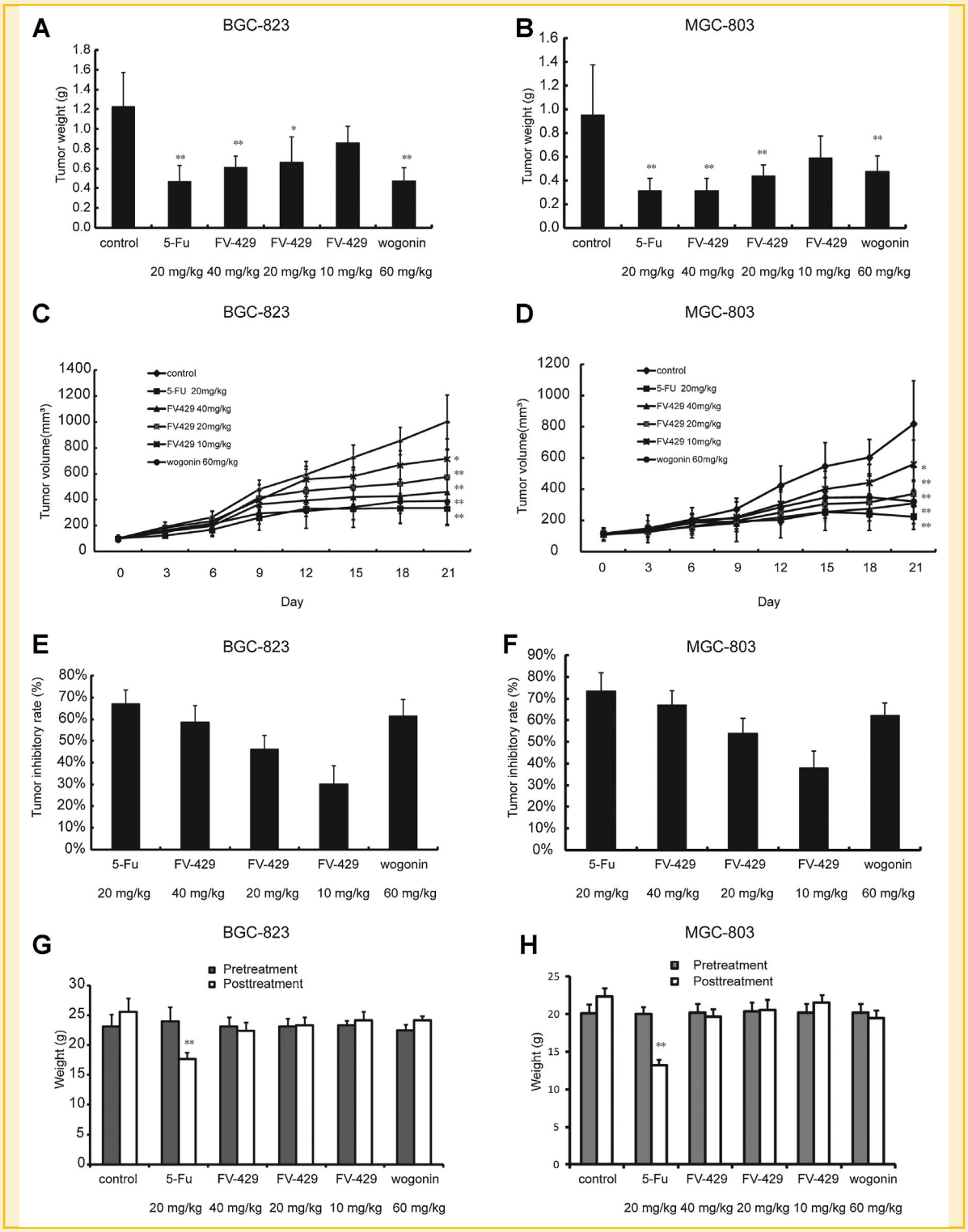

Fig. 7. Antitumor effects of HQS-3 in vivo. A: In the nude mice inoculated with BGC-823 cells, tumor weight of control, 5-Fu (20 mg/kg), FV-429 (40, 20, and 10 mg/kg) and wogonin (60 mg/kg) treatment groups on BGC-823 cells. The tumor were isolated and weighed after 21 days treatment. B: In the nude mice inoculated with MGC-803 cells, tumor weight of control, 5-Fu (20 mg/kg), FV-429 (40, 20 and 10 mg/kg) and wogonin (60 mg/kg) treatment groups on MGC-803 cells. The tumor were isolated and weighed after 21 days treatment. C: The body weight of pre-dose and post-dose of the nude mice inoculated with BGC-823 cells. D: The body weight of pre-dose and post-dose of the nude mice inoculated with MGC-803 cells. E: The tumor inhibitory rate of 5-Fu, FV-429 and wogonin groups on BGC-823 cells. Each data point is the average from six mice. F: The tumor inhibitory rate of 5-Fu, FV-429 and wogonin groups on MGC-803 cells. Each data point is the average from six mice. (G) In the nude mice inoculated with BGC-823 cells, tumor volume of control, 5-Fu (20 mg/kg), FV-429 (40, 20, and 10 mg/kg) and wogonin (60 mg/kg) treatment groups. Tumor sizes were measured once every 3 days. (H) In the nude mice inoculated with MGC-803 cells, tumor volume of control, 5-Fu (20 mg/kg), FV-429 (40, 20, and 10 mg/kg) and wogonin (60 mg/kg) treatment groups. Tumor sizes were measured once every 3 days.

66.99%, 53.99% and 37.84%, respectively. However, the advantage of FV-429 upon wogonin is that it induces the same biological effect as wogonin at much lower concentrations. Meanwhile, compared with control, FV-429 had no significant influence on the body weight.

Apoptosis is controlled by a diverse range of cell signals which may originate intracellularly or extracellularly [Sola et al., 2013]. The proteins of the bcl-2 family are of special importance to mitochondrial-mediated apoptosis [Xu et al., 2013]. Anti-apoptotic protein bcl-2 acts as a repressor of apoptosis, whereas pro-apoptotic protein Bax acts as a promoter [Faiao-Flores et al., 2013]. FV-429 treatment resulted in an obvious decrease in Bcl-2 protein expression and a notable increase in Bax protein production in BGC-823 and MGC-803 cells. It is therefore postulated that FV-429′s efficient inhibitory effect on tumor cell growth is achieved by its ability to modulate the expression of Bcl-2/Bax proteins that are involved in the regulation of apoptosis.

Besides the ratio between Bcl-2 and Bax, ROS also appears to be a central event in the apoptosis [Quast et al., 2013]. Moreover, ROS was recently shown to induce apoptosis by regulating phosphorylation and activation of the MAPK pathways, resulting in increased proapoptotic protein levels and decreased antiapoptotic protein expression, with subsequent cell death [Chen et al., 2013]. Our study showed that FV-429-induced apoptosis involves ROS generation. Here in the present study, we found two intracellular ROS, superoxide, and hydrogen peroxide were elevated immediately following FV-429 exposure.

As to the detailed mechanism how ROS mediates apoptosis, we found ERK played a significant role. ERK2 was translocated into the nucleus under the regulation of ROS, therefore we infer ERK2 probably entered the nucleus to phosphorylate and activate one or more transcription factors. As a vital tumor suppressor, p53 exerted its antitumor effects mainly by transactivation of diverse target genes including Bax, Apaf-1 and caspase-6, or to induce apoptosis independent of its transactivation ability [Wallace and Cotter, 2009; Chiu et al., 2013; Ngok-Ngam et al., 2013]. Collectively, these results indicated that by virtue of nuclear translocation, ERK2 phosphorylated and activated p53 in the nucleus. We also found p53 translocated into the nucleus accompanied with the translocation of ERK2.

Taken together, the present study demonstrated that FV-429 could induce the mitochondrial-mediated apoptotic pathway, increase ROS and activate the MAPK pathway in BGC-823 and MGC-803 cells. Moreover we found that FV-429 increased ROS leads to ERK2 translocation, resulting in the activation of p53 in the nucleus and p53-mediated apoptosis. In conclusion, FV-429 holds promise for further development as a potential antitumor agent for GC.

ACKNOWLEDGMENTS

This work was supported by the Project Program of State Key Laboratory of Natural Medicines, China Pharmaceutical University (No. JKGZ201101, SKLNMZZ201210, SKLNMZZCX201303 and SKLNMZZJQ201302), the Natural Science Foundation of China (No.30973556, No. 91029744 and No.81173086), Natural Science Foundation of Jiangsu Province (BK2011620), the National Science & Technology Major Project (No.2012ZX09304-001) and Program for Changjiang Scholars and Innovative Research Team in University (PCSIRT-IRT1193).

REFERENCES

Aiyegoro OA, Okoh AI. 2009. Phytochemical screening and polyphenolic antioxidant activity of aqueous crude leaf extract of Helichrysum pedunculatum. Int J Mol Sci 10:4990–5001.

Benz CC, Yau C. 2008. Ageing, oxidative stress and cancer: Paradigms in parallax. Nat Rev Cancer 8:875–879.

Bobyleva V, Pazienza TL, Maseroli R, Tomasi A, Salvioli S, Cossarizza A, Franceschi C, Skulachev VP. 1998. Decrease in mitochondrial energy coupling by thyroid hormones: A physiological effect rather than a pathological hyperthyroidism consequence. FEBS Lett 430:409–413.

Celotto AM, Liu Z, Vandemark AP, Palladino MJ. 2012. A novel Drosophila SOD2 mutant demonstrates a role for mitochondrial ROS in neurodevelopment and disease. Brain Behav 2:424–434.

Chen CY, Chen YK, Wang JJ, Hsu CC, Tsai FY, Sung PJ, Lin HC, Chang LS, Hu WP. 2013. DC-81-enediyne induces apoptosis of human melanoma A375 cells: Involvement of the ROS, p38 MAPK, and AP-1 signaling pathways. Cell Biol Toxicol 29:85–99.

Chiu TH, Lan KY, Yang MD, Lin JJ, Hsia TC, Wu CT, Yang JS, Chueh FS, Chung JG. 2013. Diallyl sulfide promotes cell-cycle arrest through the p53 expression and triggers induction of apoptosis via caspase- and mitochondria-dependent signaling pathways in human cervical cancer Ca Ski cells. Nutr Cancer 65:505–514.

Das A, Gopalakrishnan B, Voss OH, Doseff AI, Villamena FA. 2012. Inhibition of ROS-induced apoptosis in endothelial cells by nitrone spin traps via induction of phase II enzymes and suppression of mitochondria-dependent pro-apoptotic signaling. Biochem Pharmacol 84:486–497.

Das M, Ray PK. 1988. Lipid antioxidant properties of quercetin in vitro. Biochem Int 17:203–209.

el-Deiry WS. 1998. Regulation of p53 downstream genes. Semin Cancer Biol 8:345–357.

Faiao-Flores F, Coelho PR, Toledo Arruda-Neto JD, Maria-Engler SS, Tiago M, Capelozzi VLM, Giorgi RR, Maria DA. 2013. Apoptosis through Bcl-2/Bax and cleaved caspase up-regulation in melanoma treated by boron neutron capture therapy. PLoS One 8:e59639.

Fazal F, Gu L, Ihnatovych I, Han Y, Hu W, Antic N, Carreira F, Blomquist JF, Hope TJ, Ucker DS, de Lanerolle P. 2005. Inhibiting myosin light chain kinase induces apoptosis in vitro and in vivo. Mol Cell Biol 25:6259–6266.

Ferlay J, Shin HR, Bray F, Forman D, Mathers C, Parkin DM. 2010. Estimates of worldwide burden of cancer in 2008: GLOBOCAN 2008. Int J Cancer 127:2893–2917.

Gabor M. 1986. Anti-inflammatory and anti-allergic properties of flavonoids. Prog Clin Biol Res 213:471–480.

Garcia-Tirado J, Rieger-Reyes C, Saz-Peiro P. 2012. Effect of flavonoids in the prevention of lung cancer: Systematic review. Med Clin (Barc) 139: 358–363.

Gilman AG, Simon MI, Bourne HR, Harris BA, Long R, Ross EM, Stull JT, Taussig R, Bourne HR, Arkin AP, Cobb MH, Cyster JG, Devreotes PN, Ferrell JE, Fruman D, Gold M, Weiss A, Stull JT, Berridge MJ, Cantley LC, Catterall WA, Coughlin SR, Olson EN, Smith TF, Brugge JS, Botstein D, Dixon JE, Hunter T, Lefkowitz RJ, Pawson AJ, Sternberg PW, Varmus H, Subramaniam S, Sinkovits RS, Li J, Mock D, Ning Y, Saunders B, Sternweis PC, Hilgemann D, Scheuermann RH, DeCamp D, Hsueh R, Lin KM, Ni Y, Seaman WE, Simpson PC, O′Connell TD, Roach T, Simon MI, Choi S, Eversole-Cire P, Fraser I, Mumby MC, Zhao Y, Brekken D, Shu H, Meyer T, Chandy G, Heo WD, Liou J, O′Rourke N, Verghese M, Mumby SM, Han H, Brown HA, Forrester JS, Ivanova P, Milne

SB, Casey PJ, Harden TK, Arkin AP, Doyle J, Gray ML, Meyer T, Michnick S, Schmidt MA, Toner M, Tsien RY, Natarajan M, Ranganathan R, Sambrano GR. Participating i, scientists of the Alliance for Cellular S. 2002. Overview of the Alliance for Cellular Signaling. Nature 420:703–706.

Havsteen BH. 1984. Linear free energy relationship for osmotic water flow through a membrane. Biophys Chem 20:305–317.

Hayakawa Y, Hirata Y, Sakitani K, Nakagawa H, Nakata W, Kinoshita H, Takahashi R, Takeda K, Ichijo H, Maeda S, Koike K. 2012. Apoptosis signal-regulating kinase-1 inhibitor as a potent therapeutic drug for the treatment of gastric cancer. Cancer Sci 103:2181–2185.

Jalving M, de Jong S, Koornstra JJ, Boersma-van Ek W, Zwart N, Wesseling J, de Vries EG, Kleibeuker JH. 2006. TRAIL induces apoptosis in human colorectal adenoma cell lines and human colorectal adenomas. Clin Cancer Res 12:4350–4356.

Jiang C, Hu H, Malewicz B, Wang Z, Lu J. 2004. Selenite-induced p53 Ser-15 phosphorylation and caspase-mediated apoptosis in LNCaP human prostate cancer cells. Mol Cancer Ther 3:877–884.

Kandaswami C, Middleton E Jr. 1994. Free radical scavenging and antioxidant activity of plant flavonoids. Adv Exp Med Biol 366:351–376.

Kerr JF, Wyllie AH, Currie AR. 1972. Apoptosis: A basic biological phenomenon with wide-ranging implications in tissue kinetics. Br J Cancer 26:239–257.

Lakin ND, Jackson SP. 1999. Regulation of p53 in response to DNA damage. Oncogene 18:7644–7655.

Lane DP, Lu X, Hupp T, Hall PA. 1994. The role of the p53 protein in the apoptotic response. Philos Trans R Soc Lond B Biol Sci 345:277–280.

Lenz HJ. 2004. Angiogenesis as a target in colorectal cancer therapy. Introduction. Semin Oncol 31:1–2.

Li HN, Nie FF, Liu W, Dai QS, Lu N, Qi Q, Li ZY, You QD, Guo QL. 2009. Apoptosis induction of oroxylin A in human cervical cancer HeLa cell line in vitro and in vivo. Toxicology 257:80–85.

Li Z, Shi K, Guan L, Cao T, Jiang Q, Yang Y, Xu C. 2010. ROS leads to MnSOD upregulation through ERK2 translocation and p53 activation in selenite-induced apoptosis of NB4 cells. FEBS Lett 584:2291–2297.

Lin CC, Kuo CL, Lee MH, Lai KC, Lin JP, Yang JS, Yu CS, Lu CC, Chiang JH, Chueh FS, Chung JG. 2011. Wogonin triggers apoptosis in human osteosarcoma U-2 OS cells through the endoplasmic reticulum stress, mitochondrial dysfunction and caspase-3-dependent signaling pathways. Int J Oncol 39:217–224.

Liu H, Xiao Y, Xiong C, Wei A, Ruan J. 2011. Apoptosis induced by a new flavonoid in human hepatoma HepG2 cells involves reactive oxygen species-mediated mitochondrial dysfunction and MAPK activation. Eur J Pharmacol 654:209–216.

Liu HL, Jiang WB, Xie MX. 2010. Flavonoids: Recent advances as anticancer drugs. Recent Pat Anticancer Drug Discov 5:152–164.

Liu T, Hannafon B, Gill L, Kelly W, Benbrook D. 2007. Flex-Hets differentially induce apoptosis in cancer over normal cells by directly targeting mitochondria. Mol Cancer Ther 6:1814–1822.

Meek DW. 1999. Mechanisms of switching on p53: A role for covalent modification? Oncogene 18:7666–7675.

Middleton E Jr, Kandaswami C, Theoharides TC. 2000. The effects of plant flavonoids on mammalian cells: Implications for inflammation, heart disease, and cancer. Pharmacol Rev 52:673–751.

Morgan SE, Kastan MB. 1997. p53 and ATM: Cell cycle, cell death, and cancer. Adv Cancer Res 71:1–25.

Ngok-Ngam P, Watcharasit P, Thiantanawat A, Satayavivad J. 2013. Pharmacological inhibition of GSK3 attenuates DNA damage-induced apoptosis via reduction of p53 mitochondrial translocation and Bax oligomerization in neuroblastoma SH-SY5Y cells. Cell Mol Biol Lett 18:58–74.

Nirmalan NJ, Harnden P, Selby PJ, Banks RE. 2009. Development and validation of a novel protein extraction methodology for quantitation of protein expression in formalin-fixed paraffin-embedded tissues using Western blotting. J Pathol 217:497–506.

Ott K, Lordick F, Blank S, Buchler M. 2011. Gastric cancer: Surgery in 2011. Langenbecks Arch Surg 396:743–758.

Pedrazzani C. 2011. Functional outcomes after extended surgery for gastric cancer. Br J Surg 98:239–246.

Pick A, Muller H, Mayer R, Haenisch B, Pajeva IK, Weigt M, Bonisch H, Muller CE, Wiese M. 2011. Structure-activity relationships of flavonoids as inhibitors of breast cancer resistance protein (BCRP). Bioorg Med Chem 19:2090–2102.

Qiang L, Yang Y, You QD, Ma YJ, Yang L, Nie FF, Gu HY, Zhao L, Lu N, Qi Q, Liu W, Wang XT, Guo QL. 2008. Inhibition of glioblastoma growth and angiogenesis by gambogic acid: An in vitro and in vivo study. Biochem Pharmacol 75:1083–1092.

Quast SA, Berger A, Eberle J. 2013. ROS-dependent phosphorylation of Bax by wortmannin sensitizes melanoma cells for TRAIL-induced apoptosis. Cell Death Dis 4:e839.

Reed JC. 2000. Mechanisms of apoptosis. Am J Pathol 157:1415–1430.

Romagnolo DF, Selmin OI. 2012. Flavonoids and cancer prevention: A review of the evidence. J Nutr Gerontol Geriatr 31:206–238.

Sano T, Sasako M, Yamamoto S, Nashimoto A, Kurita A, Hiratsuka M, Tsujinaka T, Kinoshita T, Arai K, Yamamura Y, Okajima K. 2004. Gastric cancer surgery: Morbidity and mortality results from a prospective randomized controlled trial comparing D2 and extended para-aortic lymphadenectomy – Japan Clinical Oncology Group study 9501. J Clin Oncol 22:2767–2773.

Shi Y, Sahu RP, Srivastava SK. 2008. Triphala inhibits both in vitro and in vivo xenograft growth of pancreatic tumor cells by inducing apoptosis. BMC Cancer 8:294.

Shieh SY, Ikeda M, Taya Y, Prives C. 1997. DNA damage-induced phosphorylation of p53 alleviates inhibition by MDM2. Cell 91:325–334.

Siliciano JD, Canman CE, Taya Y, Sakaguchi K, Appella E, Kastan MB. 1997. DNA damage induces phosphorylation of the amino terminus of p53. Genes Dev 11:3471–3481.

Sola S, Morgado AL, Rodrigues CM. 2013. Death receptors and mitochondria: Two prime triggers of neural apoptosis and differentiation. Biochim Biophys Acta 1830:2160–2166.

Sugimoto T, Okamoto M, Mitsuno Y, Kondo S, Ogura K, Ohmae T, Mizuno H, Yoshida S, Isomura Y, Yamaji Y, Kawabe T, Omata M, Koike K. 2012. Endoscopic submucosal dissection is an effective and safe therapy for early gastric neoplasms: A multicenter feasible study. J Clin Gastroenterol 46:124–129.

Trachootham D, Alexandre J, Huang P. 2009. Targeting cancer cells by ROS-mediated mechanisms: A radical therapeutic approach? Nat Rev Drug Discov 8:579–591.

Van Laethem A, Nys K, Van Kelst S, Claerhout S, Ichijo H, Vandenheede JR, Garmyn M, Agostinis P. 2006. Apoptosis signal regulating kinase-1 connects reactive oxygen species to p38 MAPK-induced mitochondrial apoptosis in UVB-irradiated human keratinocytes. Free Radic Biol Med 41: 1361–1371.

Wagner AD, Grothe W, Haerting J, Kleber G, Grothey A, Fleig WE. 2006. Chemotherapy in advanced gastric cancer: A systematic review and meta-analysis based on aggregate data. J Clin Oncol 24:2903–2909.

Wallace DM, Cotter TG. 2009. Histone deacetylase activity in conjunction with E2F-1 and p53 regulates Apaf-1 expression in 661W cells and the retina. J Neurosci Res 87:887–905.

Wang M, Zhang L, Han X, Yang J, Qian J, Hong S, Samaniego F, Romaguera J, Yi Q. 2007. Atiprimod inhibits the growth of mantle cell lymphoma in vitro and in vivo and induces apoptosis via activating the mitochondrial pathways. Blood 109:5455–5462.

Wang W, Guo QL, You QD, Zhang K, Yang Y, Yu J, Liu W, Zhao L, Gu HY, Hu Y, Tan Z, Wang XT. 2006. The anticancer activities of wogonin in murine sarcoma S180 both in vitro and in vivo. Biol Pharm Bull 29:1132–1137.

Xu J, Zhou M, Ouyang J, Wang J, Zhang Q, Xu Y, Xu X, Zeng H. 2013. Gambogic acid induces mitochondria-dependent apoptosis by modulation of Bcl-2 and Bax in mantle cell lymphoma JeKo-1 cells. Chin J Cancer Res 25:183–191.

Yang Z, Qiang L, Wu T, Chen FH, Yang HY, Zhao Q, Zou MJ, Sun YJ, Li ZY, Guo QL. 2011. Reactive oxygen species-mitochondria pathway involved in FV-429-induced apoptosis in human hepatocellular carcinoma HepG2 cells. Anticancer Drugs 22:886–895.

Yu JQ, Liu HB, Tian DZ, Liu YW, Lei JC, Zou GL. 2007. Changes in mitochondrial membrane potential and reactive oxygen species during wogonin-induced cell death in human hepatoma cells. Hepatol Res 37: 68–76.